Mixing of Liquids in Microfluidic Devices

Bruce A. Finlayson*[1], Andy Aditya[1], Vann Brasher[1], Lisa Dahl[1], Ha Quan Dinh[1], Adam Field[1], Jordan Flynn[1], Curtis Jenssen[1], Daniel Kress, [1] Anna Moon[1], Francis Ninh[1], Andrew Nordmeier[1], Ho Hack Song[1], and Cindy Yuen[1]
[1]University of Washington
*Corresponding author: Dept. Chem. Engr., Box 351750, University of Washington, Seattle, WA 98115

Abstract: The mixing of liquids was characterized in thirteen different microfluidic devices. The goal was to characterize in a uniform manner the flow and mixing that occurred in slow, laminar flow and to present the results that allow quick designs. The mixing of a dilute chemical in another liquid during slow, laminar flow is a particularly difficult task, but the results showed that for Reynolds number of 1.0 (appropriate to microfluidics) the amount of mixing depended mainly on the flow length divided by the Peclet number, for all geometries. Two-dimensional simulations frequently gave a good approximation of the three-dimensional simulations, and the optical variance (as measured by fluorescence) is not too different from the flow variance (sometimes called the mixing cup variance). All simulations were done using Comsol Multiphysics using the Navier-Stokes equation and the convective diffusion equation.

Keywords: microfluidics, mixing, diffusion

1. Introduction

When designing a microfluidic device, it is important to be able to mix chemicals quickly and easily. One method is to have active mixing, such as with a stirrer. The other alternative it passive mixing, in which the mixing takes place because of the fluid flow induced by the microfluidic device. We concentrate on the latter. One type of passive mixers is a 'split and recombine' mixer, in which streams of different concentrations are brought into contact so that diffusion can take place between them, and then they are separated and brought together in a different way to speed up the process. Another type is a chaotic mixer in which the fluid is divided into lamellae that are woven together. Both types are reviewed in the literature [1, 7, 13, 15]. Here we characterize thirteen different passive mixers. The most successful of those include the herringbone mixer [16, 19] and serpentine mixer [2, 12]. The herringbone mixer has been characterized extensively and is not considered here except to note that the mixing depends chiefly on z'/Pe [19], which is the same conclusion for the mixers treated below.

The study is focused on situations with passive mixers (i.e. no mechanical mixing) at low Reynolds numbers. For a few of the geometries, inertial effects (at higher Reynolds numbers) are explored. Special geometries are necessary for this to be effective. Questions addressed for each geometry are:

A. Do the variances collapse onto one curve if properly presented?
B. Do the results follow the same curve of variance vs. z'/Pe as for a T-sensor?
C. How different are the mixing cup and optical variances? Is this difference important?
D. How do 2D and 3D results compare?
E. What is needed for each device to reach a variance of 0.01? 0.001?
F. What is the effect of Reynolds number? (This is pertinent only to a few of the geometries.)
G. What is the trade-off of decreasing variance and increasing pressure drop?

2. Use of COMSOL Multiphysics

The equations are solved in non-dimensional form. The 2D and 3D Navier-Stokes equation and convective diffusion equation (CD) are:

$$\mathbf{u}\cdot\nabla\mathbf{u} = -\nabla p' + \frac{1}{Re}\nabla^2\mathbf{u},$$

$$\mathbf{u}\cdot\nabla c = \frac{1}{Pe}\nabla^2\mathbf{u}$$

$$Re = \frac{\rho u_s x_s}{\eta},\ Pe = \frac{u_s x_s}{D}, Sc = \frac{\nu}{D}, Pe = ReSc$$

The choices of characteristic velocity, u_s, and characteristic distance, x_s, are specified below for each geometry. Generally they are an average velocity and a diameter or thickness, respectively. Boundary conditions for flow are no slip on the solid walls, specified velocity profile on the inlet boundary, and assigned pressure on the outlet boundary. The boundary

conditions for the CD equation are zero flux on solid walls and convective flux on the outlet boundary. If there is a single entry port, the concentration is zero in one half and 1.0 in the other half. If there are two entry ports in the geometry, the concentration is zero in one and 1.0 in the other; thus, the average concentration in each device is 0.5. The Peclet number was varied from 10 to 1000. All simulations were done in Comsol Multiphysics, v. 3.4. by first solving the Navier-Stokes equations and then solving the CD equation for Peclet numbers from 10 to 1000. The size of the problem varied with geometry: 30,000 to 60,000 elements giving 150,000 to 300,000 degrees of freedom for the Navier-Stokes equation and 75,000 to 150,000 degrees of freedom for the CD equation.

The variance at the exit was calculated using

$$\sigma^2_{mixingcup} = \int_A [c-0.5]^2 \mathbf{u}\bullet\mathbf{dA} \,/\, \int_A \mathbf{u}\bullet\mathbf{dA}$$

If the velocity variable is left out of the above formulas, one gets the variance that one would measure with optical fluorescence integrated through the device.

The pressure drop is computed from the total pressure drop in the simulations, $\Delta p'$.

$$\Delta p(Pa) = \rho u_s^2 \Delta p'$$

For comparison purposes, we use water as the carrier fluid, so that ρ = 1000 kg/m^3 and η =0.001 Pa s. The base case velocity is taken as 0.005 m s^{-1} and the characteristic dimension was taken as 200 μ. This gives a Reynolds number of 1.0. When *Pe* = 1000, the diffusivity is

$$D = \frac{x_s u_s}{1000} = 10^{-9}\,\mathrm{m}^2$$

This is a reasonable value for typical organic chemicals, but biological molecules usually have smaller values, perhaps by a factor of 10-100. However, this was as low as we could go given the computer equipment available. Going to higher Peclet numbers requires a much finer mesh, which necessitates more memory that was available. However, as we see below, it is possible to predict the mixing for higher Peclet numbers based on calculations in shorter devices with lower Peclet numbers. This was tested, at least, within the range of $10 \le Pe \le 1000$.

3. Analytical Theory

The significance of different levels of variance is demonstrated in Figure 1 by calculating the variance for different concentration distributions in a T-sensor [8], which is illustrated in Figure 2. Flow comes in the two ports on the left and exits on the right. Diffusion occurs across the mid-plane in the device.

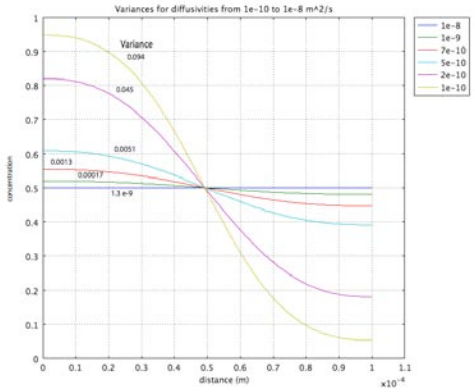

Figure 1. Concentration profiles leading to different variances. Average concentration 0.5; velocity profile is parabolic.

In work published previously [6] the T-sensor is characterized as shown in Figure 3. Note that the variance roughly follows one curve, regardless of the Peclet number, provided the results are plotted versus z'/Pe. This is expected because the flow is basically straight down the device, except for the short entrance region, with diffusion sideways, and there is no convection sideways. Thus, diffusion controls the mixing, and the time in the device determines how far the material can diffuse. The parameter

$$\frac{z'}{Pe} = \frac{z}{x_s}\frac{D}{u_s x_s} = \frac{z/u_s}{x_s^2/D} = \frac{t_{flow}}{t_{diffusion}}$$

thus is a ratio of the characteristic time for flow in the axial direction to the time for diffusion in

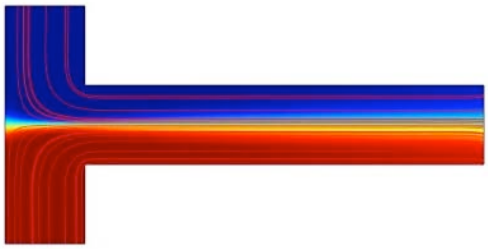

Figure 2. T-sensor; lines are streamlines, color is concentration (red = 1, blue = 0)

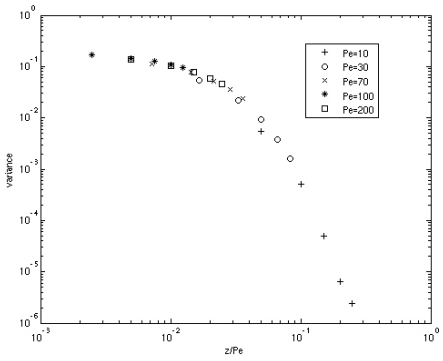

Figure 3. Variance of T-sensor for *Re* = 1; [6, using different definitions than the other figures]

the transverse direction. Alternatively, one can examine the convective diffusion equation when there is no transverse velocity

$$w(x,y)\frac{\partial c}{\partial z} = D\left[\frac{\partial^2 c}{\partial x^2} + \frac{\partial^2 c}{\partial y^2} + \frac{\partial^2 c}{\partial z^2}\right]$$

and argue that axial diffusion term, $D\partial^2 c / \partial z^2$, can be neglected compared with the axial convection term, $w\partial c / \partial z$, since their ratio is proportional to 1/*Pe*.

To further validate this concept in 3D, Figure 4a shows a geometry with two pipes joining, and Figure 4b shows the variance as a function of z'/Pe; data for the T-sensor and the two pipes joining essentially superimpose on each other.

An approximation to the variance can be derived analytically using the Method of Weighted Residuals [5] for the case of a uniform velocity. (See the Appendix).

$$\sigma^2 = \begin{cases} 0.25\left(1 - 1.476\sqrt{2z'/Pe}\right), & z'/Pe \le 0.05 \\ 0.220\exp(-10z'/Pe), & z'/Pe > 0.05 \end{cases}$$

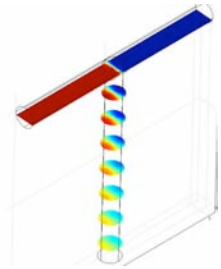

Figure 4a. Two pipes joining

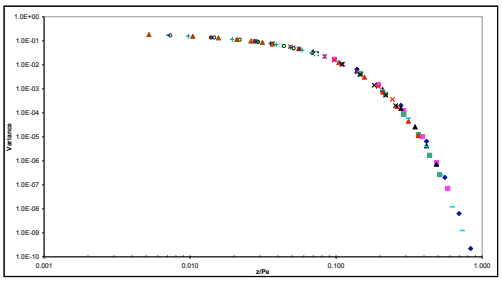

Figure 4b. Variance of mixing with two pipes joining (3D)and a 2D T-sensor, variety of *Re, Pe*, and dimensions; using different definitions than in other figures.

In this formula, the characteristic distance is the total width of the T-sensor and the velocity is the inlet average velocity. It is plotted below on the composite graphs. For comparison, a finite difference solution was used. For a flat velocity profile, the approximate solution and finite difference solution for 20 and 40 points superimpose in Figure 5. When the velocity profile is quadratic (for fully developed flow between two flat plates) the variance is slightly smaller.

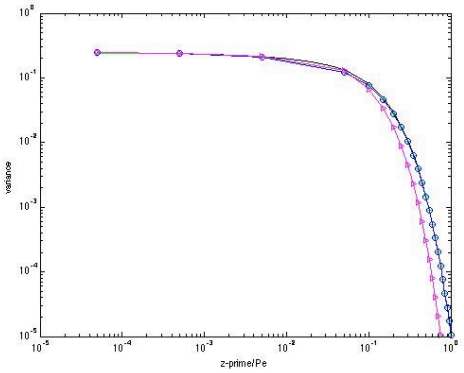

Figure 5. Variance for T-sensor
o – finite difference results and approximate solution, flat velocity profile; triangle – finite difference results with quadratic velocity profile

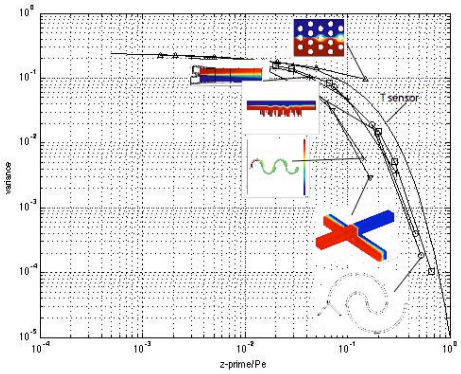

Figure 6. Variance for devices like the T-sensor

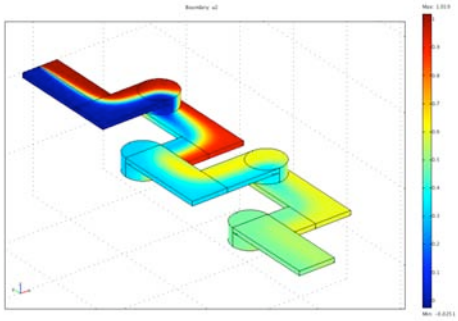

Figure 7a. Serpentine Mixer

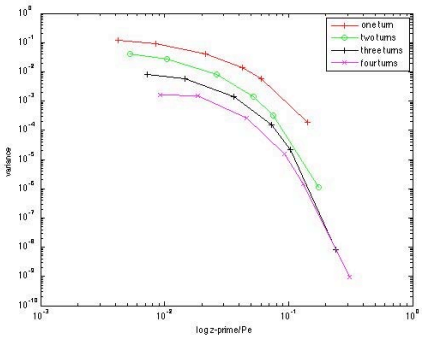

Figure 7b. Variances for serpentine mixer

4. Results

In addition to the T-sensor and two pipes joining, a variety of devices were examined. The devices are listed in Table 1 and typical concentration profiles are illustrated in the figures below. First consider the devices that are modest extensions of the T-sensor, with roughly parallel flow. They include sandwich device [9], a planar spiral [17], a rectangular expansion in a spiral [18], a rough channel [11], flow past pillars, and crossed channels [14]. Figure 6

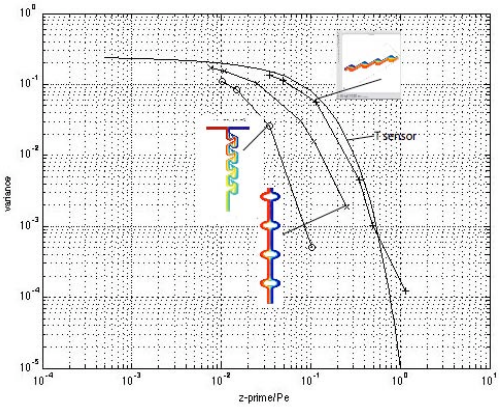

Figure 8. Variance for inertial devices

shows the variance for these devices, with a picture illustrating the shape.

Another example of mixing is for the serpentine mixer [2, 6, 12]. Figure 7a shows a typical concentration profile. In this case, enhanced mixing occurs due to the flow irregularities, even for a Reynolds number of 1.0. As shown elsewhere [6] the serpentine mixer can be several hundred times shorter to achieve the same mixing as in a T-sensor. The progress of the mixing is shown step by step in Figure 7b. Now the curves do not superimpose, but the general shape of them is similar.

Some devices have been proposed that use fluid flow that occurs mainly at higher Reynolds number than used here to create vortices. These include mixing chambers [4], tesla mixers [10], and tear drop mixers [3]. The Reynolds number must be significantly higher, though. The variance for those devices for $Re = 1$ are shown in Figure 8.

While not shown here, other results [20] show that the optical variance is almost the same as the mixing cup variance, on the scale of the log-log graphs. In addition, if a 3D object is made simply by extruding a 2D pattern in the third direction, the variance follows roughly the same curve. Another feature that is relevant is the pressure drop needed to achieve the flow. Since the Reynolds number is small (1.0) the pressure drop is directly proportional to velocity; the pressure drops are shown in Table 1 for the standard conditions (water at 0.005 m/s). If the length is increased, to decrease the variance, the variance fall much more quickly than the pressure drop increases; thus, a relative advantage is gained by lengthening the device.

5. Conclusion

The variance for each geometry, for Re = 1, fell on one curve as a function of z'/Pe. After an entry region, the variance decreased exponentially. The curve was similar in all cases, but shifted a bit for each device, and the approximate solution for a T-sensor gives an upper bound for the variance. The optical variances differed from the mixing cup variance insignificantly on a logarithmic scale. Oftentimes the 2D simulations give a good representation of the 3D simulations; the case when this doesn't hold is when the flow is particularly 3D in nature. With these 'universal curves', it is possible to design a device to achieve a predetermined mixing level without doing numerical simulations, or at least doing the numerical simulations only for the best designs.

8. References

1. Aref, H., "Stirring by Chaotic Advection," *J. Fluid Mech.* **143** 1-21 (1984).

2. Beebe, D. J., Adrian, R. J., Olsen, M. G., Stremler, M. A., Aref, H., Ho, B. H., "Passive mixing in microchannels: Fabrication and flow experiments," *Mec. Ind.* **2** 343-348 (2001).

3. Bown, M., MacInnes, J., Vikhansky, A., Allen, R., Bom, M., University of Sheffield, www,micronit.com.

4. Chung, Y. C., Hsu, Y. L, Jen, C. P., Lu, M. C., Lin, Y. C., "Design of passive mixers utilizsing microfluidic self-circulation in the mixing chamber," *Lab Chip* **4** 70-77 (2004).

5. Finlayson, B. A., *Nonlinear Analysis in Chemical Engineering,* McGraw-Hill (1980); Ravenna Park (2003).

6. Finlayson, Bruce A., Pawel W. Drapala, Matt Gebhardt, Michael D. Harrison, Bryan Johnson, Marlina Lukman, Suwimol Kunaridtipol, Trevor Plaisted, Zachary Tyree, Jeremy VanBuren, Albert Witarsa, "Micro-component flow characterization," Ch. 8 in Micro-Instrumentation, (M. Koch, K.Vanden Bussche, R. Chrisman (ed.), Wiley, 2007).

7. Hardt, S., "Microreactors – Modeling and Simulation," Article in *Ullmann's Encylopedia of Industrial Chemistry*, (2006).

8. Hatch, A., Kamholz, A. E., Hawkins, K. R., Munson, M. S., Schilling, E. A., Weigl, B. H., Yager, P., "A rapid diffusion immunoassay in a T-sensor," *Nature Biotechnology* **19**, 461 - 465 (2001).

9. Hinsmann, P., Frank, J., Svasek, P., Harasek, M., Lendl, B., "Design, simulation and application of a new micromixing device for time resolved infrared spectroscopy of chemical reactions in solution," *Lab Chip* **1** 16-21 (2001).

10. Hong, C. C., Choi, J. W., Ahn, C. H., "A novel in-plane passive microfluidic mixer with modified Tesla structures," *Lab Chip* **4** 109-113 (2004).

11. Koplik, J., Ippolito, I., Hulin, J. P., "Tracer dispersion in rough channels: A two-dimensional numerical study," *Phys. Fluids A* **5** 1333-1343 (1993).

12. Neils, Christopher, Zachary Tyree, Bruce Finlayson, Albert Folch, "Combinatorial mixing of microfluidic streams", Lab-on-a-Chip 4 342-350 (2004).

13. Ottino, J. M., *The Kinematics of Mixing: Stretching, Chaos, and Transport,*, Cambridge Univ. Press, Cambridge (1989).

14. Phelan, F. R., Jr., Hughes, N. R., Pathak, J. A., "Chaotic mixing in microfluidic devices driven by oscillatory cross flow," *Phys. Fluids* **20** 023101 (2008).

15. Ranz, W. E., "Applications of a Stretch Model to Mixing, Diffusion, and Reaction in Laminar and Turbulent Flows," *AIChE J* **25** 41-47 (1979).

16. Stroock, A. D., Dertinger, S. K. W., Ajdarim, A., Mezic, I., Stone, H. A. and Whitesides, G. M., Chaotic Mixer for Microchannels," *Science* **295** 647-651 (2002).

17. Sudarson, A. P. and Ugaz, V. M., "Fluid mixing in planar spiral microchannels," *Lab Chip* **6** 74-82 (2006).

18. Sudarson, A. P. and Ugaz, V. M., "Multivortex micromixing," *Proc. Nat. Acad. Sci.* **103** 7228-7233 (2006).

19. Williams, M. S., Longmuir, K. J. and Yager, P., "A practical guide to the staggered herringbone mixer," *Lab Chip* 8 1121-1129 (2008).

20. http://faculty.washington.edu/finlayso/microflo/

9. Acknowledgements

All authors except for the corresponding author were undergraduate students at the University of Washington. Part of their tuition was paid by the Dreyfus Foundation through a Senior Mentor Award to Professor Finlayson.

10. Appendix

An approximate solution for diffusion in the T-sensor is developed using the Method of Weighted Residuals, as described by Finlayson [5, pp. 179-180, 190]. Notice that in Figure 1 the concentration at the midpoint remains at c = 0.5. On the right of the mid-point, the concentration is initially zero, then a diffusion zone moves from the midpoint to the edge, and then the concentration increases. Thus, we pose the following problem to represent this case. Only the case of uniform velocity is done.

The diffusion equation is solved on $x = 0$ to h (from the midpoint to the edge; thus h is the half-thickness).

$$u_{avg}\frac{\partial c}{\partial z} = D\frac{\partial^2 c}{\partial x^2}$$

With boundary conditions of $c = 0.5$ at $x = 0$ and zero flux at $x = h$, and initial conditions of $c = 0$, the problem is fully specified. It is made non-dimensional using the variables

$$\frac{\partial c}{\partial z''} = \frac{\partial^2 c}{\partial x'^2}, z'' = \frac{zD}{u_{avg}h^2}, x' = \frac{x}{h}$$

$$c(0,z'') = 0.5, c(x',0) = 0, \partial c/\partial x'(1,z'') = 0$$

For the first part of the time, the concentration is zero almost everywhere with a concentration increase at $x = 0$ to $c = 0.5$. Then a thin diffusion layer grows out towards the far wall. During this time, the approximations solution is taken as

$$c = \begin{cases} 0.5*(1-a\eta)^2, \eta < 1/a \\ 0, \eta \geq 1/a \end{cases}, \quad \eta = \frac{x'}{\sqrt{4z''}}$$

This function is substituted into the differential equation to form the residual. In the Galerkin method the residual is made orthogonal to the trial function, which in this case is the derivative of the function with respect to the unknown parameter, a. This is the same procedure that is used in the Galerkin finite element method, except that the trial function and weighting function are not finite elements here. Solving for a gives $a^2 = 2/5$. This solution holds until the diffusion front meets the wall, which is $z'' \leq 0.1$. Calculating the variance gives

$$\sigma^2 = 0.25\left(1 - 1.476\sqrt{z''}\right), z'' \leq 0.1$$

At $z'' = 0.1$ the variance is 0.133. After this time another form of the solution is used.

$$c = 0.5 + d(z'')(x'^2 - 2x')$$

The initial condition is $d(0.1) = 0.5$ to make the start of this solution agree with the end of the previous one. Substituting this formula into the differential equation forms the residual. In the Galerkin method this time the weighting function is

$$(x'^2 - 2x')$$

and the solution for d is

$$d(z") = 0.642\exp(-2.5z")$$

The variance is

$$\sigma^2 = 0.220\exp(-5z"), z" > 0.1$$

In these formulas the distance is the half-thickness and the velocity is the velocity out. In the figures shown above the total thickness is used and the velocity is the average velocity in, which is half as big. Thus, the formula for $z"$ is multiplied by 2^2 and divided by 2, giving the variance as shown in the Results section.

Table 1: Characteristics of Mixing Devices

name	pathlength	xs	delta-p (Pa)
Sandwich[1]	3	side of square	208
planar spiral[1]	104/278	width	88
rectangular expansion[2]	88	width of narrow section	6.3
rough channel[3]	20	thickness	10
pillars[3]	1.5	width	58
crossed channels[1]	5	width	8
2 pipes joining[1]		diameter	10
T-sensor[1]	5	width	3.7
mixing chamber[3]	34.7	width	14
tesla mixer[1]	10.3	width of inlet	62
tear drop[3]	7.62	width of inlet	117
serpentine[3]	5.9/9.8/13.1/21	thickness	291

1. u_s is the average velocity in one inlet
2. u_s is the average velocity in the narrow section
3. u_s is one-half the average velocity out